Title

Methane Production Pathway Regulated Proximally by Substrate Availability and Distally by Temperature in a High-Latitude Mire Complex

Journal

Journal of Geophysical Research: Biogeosciences, 124(10)

ISSN

2169-8953

Authors

Chang, KY
Riley, WJ
Brodie, EL
et al.

Publication Date

2019-10-01

DOI

10.1029/2019JG005355

Peer reviewed

Methane Production Pathway Regulated Proximally by Substrate Availability and Distally by Temperature in a High-Latitude Mire Complex

Kuang-Yu Chang[1], William J. Riley[1], Eoin L. Brodie[1], Carmody K. McCalley[2], Patrick M. Crill[3], and Robert F. Grant[4]

[1] Climate and Ecosystem Sciences Division, Lawrence Berkeley National Laboratory, Berkeley, CA, USA, [2] Thomas H. Gosnell School of Life Sciences, Rochester Institute of Technology, Rochester, NY, USA, [3] Department of Geological Sciences, Stockholm University, Stockholm, Sweden, [4] Department of Renewable Resources, University of Alberta, Edmonton, Alberta, Canada

Correspondence to: K.-Y. Chang, ckychang@lbl.gov

Abstract

Projected 21st century changes in high-latitude climate are expected to have significant impacts on permafrost thaw, which could cause substantial increases in emissions to the atmosphere of carbon dioxide (CO_2) and methane (CH_4, which has a global warming potential 28 times larger than CO_2 over a 100-year horizon). However, predicted CH_4 emission rates are very uncertain due to difficulties in modeling complex interactions among hydrological, thermal, biogeochemical, and plant processes. Methanogenic production pathways (i.e., acetoclastic [AM] and hydrogenotrophic [HM]) and the magnitude of CH_4 emissions may both change as permafrost thaws, but a mechanistic analysis of controls on such shifts in CH_4 dynamics is lacking. In this study, we reproduced observed shifts in CH_4 emissions and production pathways with a comprehensive biogeochemical model (ecosys) at the Stordalen Mire in subarctic Sweden. Our results demonstrate that soil temperature changes differently affect AM and HM substrate availability, which regulates magnitudes of AM, HM, and thereby net CH_4 emissions. We predict very large landscape-scale, vertical, and temporal variations in the modeled HM fraction, highlighting that measurement strategies for metrics that compare CH_4 production pathways could benefit from model informed scale of temporal and spatial variance. Finally, our findings suggest that the warming and wetting trends projected in northern peatlands could enhance peatland AM fraction and CH_4 emissions even without further permafrost degradation.

Plain Language Summary

Permafrost peatlands store large amounts of carbon potentially vulnerable to decomposition, and the changing climate is expected to have significant and uncertain impacts on high-latitude methane (CH_4) emissions. CH_4 is an important greenhouse gas, and CH_4 emissions represent a positive feedback with climate change. In this study, we reproduced the observed shifts in CH_4 dynamics with a comprehensive biogeochemical model (ecosys) at the

Stordalen Mire in subarctic Sweden, and quantified the effects of individual factors that regulate CH_4 dynamics. Our results show that CH_4 production rates depend on soil temperature, which itself is affected by a series of hydrological and thermal feedbacks. In addition, our results indicate that changes in soil temperature could indirectly (via substrate production) induce the measured shifts in CH_4 production pathways. Our findings suggest that the warming and wetting trends projected in high-latitude regions could enhance peatland CH_4 production rates, which could accelerate projected climate changes even without further permafrost degradation.

1 Introduction

Undecomposed soil organic carbon (SOC) stored in the northern circumpolar permafrost zone contains about twice as much carbon as currently in the atmosphere (1,460–1,600 Pg C (Hugelius et al., 2014; Schuur et al., 2015, 2018)). A significant portion of that carbon is vulnerable to be emitted as carbon dioxide (CO_2) and methane (CH_4) that have positive radiative forcing impacts as permafrost thaws (Koven et al., 2011; Schuur et al., 2015). However, estimated rates of permafrost soil carbon loss are strongly dependent on model physical and biological parameterizations that are currently very uncertain (McGuire et al., 2016, 2018). High-latitude carbon cycling is sensitive to ecosystem properties (e.g., soil moisture, soil temperature, water table position, permafrost thaw stage, microbial community, and vegetation composition), climate forcing (e.g., air temperature and precipitation), and their spatiotemporal variability (Chang et al., 2019; Malhotra & Roulet, 2015; McCalley et al., 2014; Olefeldt et al., 2013). In addition, the global radiative energy budget is sensitive to the form of permafrost soil carbon loss because the global warming potential of CH_4 is estimated to be 84 and 28 times stronger than that of CO_2 over 20 and 100 year periods, respectively (Myhre et al., 2013). Neubauer and Megonigal (2015) demonstrated that using different metrics to quantify the radiative forcing of individual greenhouse gases can yield quantitatively or even qualitatively different conclusions in global radiative energy budget estimates. Overall, the partitioning of carbon emissions between CO_2 and CH_4 is currently uncertain, and a number of knowledge gaps need to be addressed to reduce the uncertainty in global climate change assessments.

The warming and wetting trends projected in the northern circumpolar permafrost zone could enhance permafrost degradation, shift surface hydrological conditions, and thereby alter CH_4 emissions over the 21st century (Bintanja & Andry, 2017; Collins et al., 2013). Amplification of these trends at higher latitudes increases the importance of understanding these feedback connections. Studies have shown that CH_4 emissions are primarily controlled by soil microbial communities that determine CH_4 production pathways (McCalley et al., 2014; Woodcroft et al., 2018), soil thermal and moisture status that affects aerobic and anaerobic decomposition (Christensen et al., 2004; Olefeldt et al., 2013), organic matter chemistry that regulates CH_4 production rate (Hodgkins et al., 2014; Ye et al., 2012),

the relative strength between CH_4 oxidation and CH_4 production (Lofton et al., 2014; Zheng et al., 2018), and plant-mediated transport of oxygen or CH_4 through aerenchyma (Chanton, 2005; Olefeldt et al., 2013). Meta-analysis conducted by Yvon-Durocher et al. (2014) suggests that both CH_4 emissions and the ratio of CH_4 to CO_2 emissions would increase with increases in temperature. Knoblauch et al. (2018) indicated that higher global warming equivalents were formed under anaerobic conditions than under aerobic conditions through 7 year laboratory incubations. The results presented in Knoblauch et al. (2018) emphasize the importance of CH_4 production in thawing permafrost, which challenges the view of a stronger permafrost carbon feedback dominated by CO_2 production from drained (aerobic) soils (Schädel et al., 2016).

Biological CH_4 production is primarily governed by three mechanisms: acetoclastic methanogenesis (AM), hydrogenotrophic methanogenesis (HM), and methylotrophic methanogenesis (MM). MM contributes a small fraction to CH_4 emissions and is typically discounted (Penger et al., 2012). From genomic evidence, HM appears to be the most ubiquitous pathway (Thauer et al., 2008), although AM contributes most to atmospheric emissions (Fournier & Gogarten, 2008).

The proportion of CH_4 produced by AM relative to HM may increase with increasing pH (Kotsyurbenko et al., 2007), increasing organic matter reactivity (Hornibrook et al., 1997), decreasing *Sphagnum* abundance (Hines et al., 2008), and shifting microbial community response to permafrost thaw progression (Hodgkins et al., 2014; McCalley et al., 2014; Woodcroft et al., 2018). However, despite this complexity, most existing models simulate methanogenesis as a single process driven by net primary production that does not differentiate AM and HM pathways (Wania et al., 2013; Xu et al., 2016). For example, only 3 of 40 terrestrial CH_4 models reviewed in Xu et al. (2016) explicitly simulate AM and HM pathways; the relatively simple representation of CH_4 production in most models might cause significant uncertainty in CH_4 emission estimates. Deng et al. (2017) showed that the inclusion of acetate dynamics can improve estimates of CH_4 production pathways, but the mechanisms controlling the observed shifts in CH_4 cycling as permafrost thaws remain uncertain.

To build a system-level understanding of changes in CH_4 cycling, a process-based model that incorporates the above-mentioned mechanisms controlling CH_4 dynamics (i.e., soil hydrology, vegetation dynamics, acetate dynamics, and microbial dynamics) is needed. Here, we use the ecosystem scale biogeochemical model ecosys (e.g., Grant, Mekonnen, Riley, Arora, & Torn, 2017; Grant, Mekonnen, Riley, Wainwright, et al., 2017), a process-rich model that mechanically represents CH_4 dynamics, to study the shifting CH_4 cycling observed along the permafrost thaw gradient at the Stordalen Mire in subarctic Sweden (Hodgkins et al., 2014; McCalley et al., 2014; Woodcroft et al., 2018). The Stordalen Mire is in the discontinuous permafrost zone, and its landscape has been thawing over the past several decades (Christensen

et al., 2004). Permafrost thaw has expanded the areal cover of wetter sites dominated by graminoids with increased CH_4 emissions and higher AM fraction (Christensen et al., 2004; Johansson et al., 2006; McCalley et al., 2014; Mondav et al., 2014). McCalley et al. (2014) suggested that shifts in microbial community composition and CH_4 production pathways played an important role in regulating CH_4 dynamics at the Stordalen Mire, highlighting the importance of microbial ecology in ecosystem scale responses to a changing climate. We hypothesize that the observed shifts in CH_4 emission magnitude and CH_4 production pathways originate from biogeophysical feedbacks associated with permafrost thaw that triggers a series of ecosystem structural and functional responses. Specifically, we speculate that observed shifts in CH_4 dynamics are attributed to soil temperature changes resulting from changing landscape heterogeneity of vegetation cover and inundation status. We therefore address the following questions: (1) What are the factors regulating AM and HM rates along the permafrost thaw gradient (i.e., bog to fen)? (2) What are the model components necessary to reduce CH_4 production prediction uncertainty? We attempt to disentangle the interactions among biogeophysical (i.e., hydrological and thermal), biogeochemical, and plant processes to establish a basis for scaling microbial processes to ecosystem responses under a changing climate.

2 Methods and Data

2.1 Study Site Description

Our study sites are located at the Stordalen Mire (68.20°N, 19.03°E), which is about 10 km southeast of the Abisko Scientific Research Station (ANS) in northern Sweden. Continuous daily meteorological measurements have been recorded at the ANS since 1913, which are used to represent the climate conditions at our study sites. The annual mean air temperature measured at the ANS has risen by 2.5 °C from 1913 to 2006, where it exceeded the 0 °C threshold (0.6 °C in 2006) for the first time over the past century (Callaghan et al., 2010). The annual total precipitation measured at the ANS has also increased from 306 mm y^{-1} (average 1913–2009) to 336 mm y^{-1} (average 1980–2009; Olefeldt & Roulet, 2012). The annual maximum snow depth measured at the ANS has increased from 59 cm (average 1957–1971) to 70 cm (average 1986 to 2000), and the snow cover period with snow depth greater than 20 cm has decreased from 5.8 months (average 1957–1971) to 4.9 months (average 1986–2000; Malmer et al., 2005). The recent warming (more than 1 °C) has deepened the spatial mean annual maximum thaw depth (i.e., active layer depth, ALD) measured at the Stordalen Mire by about 20 cm since the early 1980s, accompanied by palsa collapses and thermokarst erosion (Christensen et al., 2004; Johansson et al., 2006; Malmer et al., 2005). Specifically, the mean ALD has increased from the 1970s to 2000s by 48–63 cm in the drier part of the mire and by 63–86 cm in the wetter part, (Johansson et al., 2006; Rydén & Kostov, 1980).

Inception of peat deposition at the Stordalen Mire has been dated at around 6,000 calibrated years before present (Sonesson, 1972) in the southern part of the mire and at around 4,700 calibrated years before present in the northern part (Kokfelt et al., 2010). At present, the Stordalen Mire can be broadly classified into three landscape types: intact permafrost palsa, partly thawed bog, and fen (Hodgkins et al., 2014), hereafter referred to as palsa, bog, and fen (Figure 1). These different permafrost thaw stages are associated with distinct hydrology (Olefeldt & Roulet, 2012), vegetation (Christensen et al., 2004; Malmer et al., 2005), microbiota (Mondav et al., 2014; Woodcroft et al., 2018), and organic matter chemistry (Hodgkins et al., 2014). The spatial distribution of these landscape types and their hydrological connections are described in (Olefeldt & Roulet, 2012). We focused our analysis in the bog and fen because the measured CH_4 exchanges were near zero in the palsa, primarily because it is drier and has a shallower ALD (Bäckstrand et al., 2008a, 2008b; Bäckstrand et al., 2010).

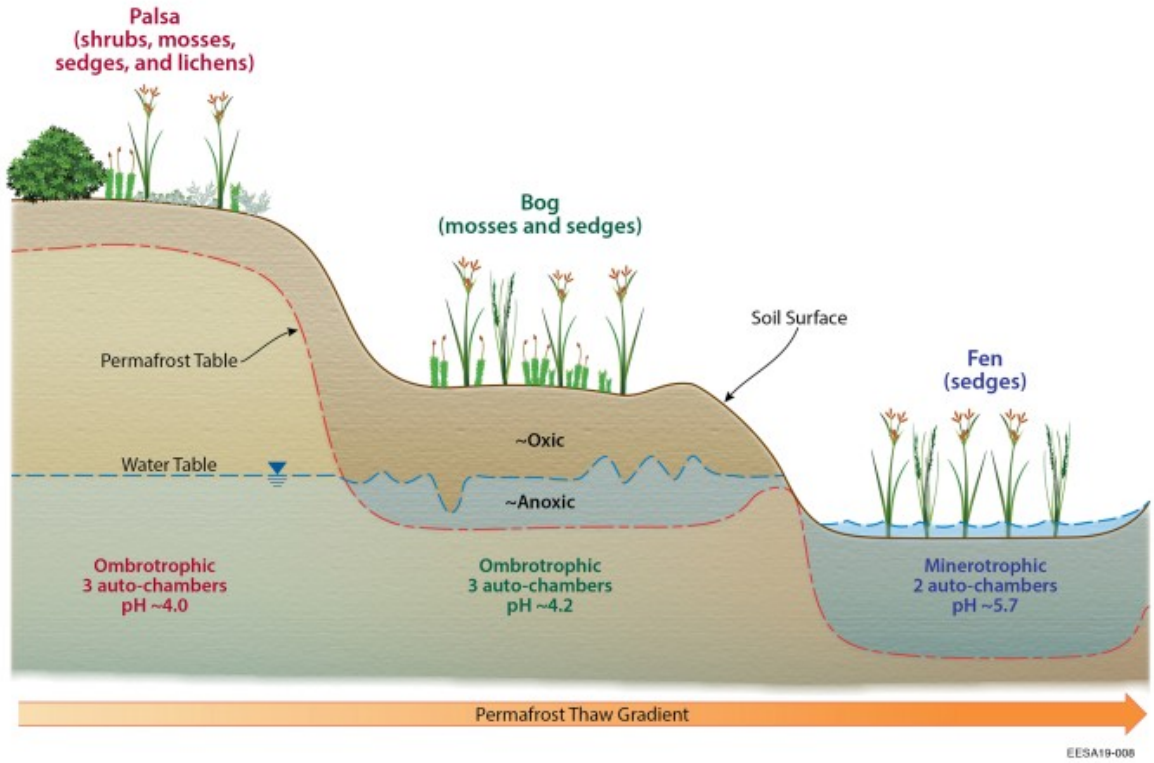

Figure 1. Schematic diagram of the sampling sites at Stordalen Mire, extracted from Chang et al. (2019). Three distinct habitats are present at the Mire: intact permafrost palsa with a shallow active layer, partly thawed bog with a deeper active layer and a variable water table, and fen with a water table near or above the peat surface. Locations of the water table are used to represent the proximate distribution of oxic and anoxic environments.

The bog is ombrotrophic (pH ~4.2) with water table depth fluctuating from the peat surface to 35 cm below the peat surface (Bäckstrand et al., 2008a, 2008b; Olefeldt & Roulet, 2012). The bog is dominated by *Sphagnum* spp. mosses with a moderate abundance of short sedges such as *Eriophorum vaginatum* and *Carex bigelowii* (Bäckstrand et al., 2008a, 2008b; Malmer et

al., 2005; Olefeldt & Roulet, 2012). The fen is minerotrophic (pH~5.7), has water table depths near or above the peat surface, receives a large amount of water from a lake directly to the east (Bäckstrand et al., 2008a, 2008b; Olefeldt & Roulet, 2012), and is dominated by tall sedges such as *E. angustifolium*, *C. rostrata*, and *Esquisetum* spp. (Bäckstrand et al., 2008a, 2008b). The bog and fen both have a peat layer ranging from 0.5 to ~1 m (Rydén & Kostov, 1980) and an ALD greater than 0.9 m (Bäckstrand et al., 2008b).

2.2 Field Measurements

Continuous daily meteorological data, including air temperature, precipitation, solar radiation, wind speed, and relative humidity, were recorded at the ANS during our study period from 2011 to 2013 (Figure S1). CH_4 gas exchanges in the bog, and fen were measured with automated chambers (three in the bog and two in the fen) during the 2011–2013 thawed seasons (McCalley et al., 2014; Mondav et al., 2014). Daily CH_4 exchange rates were derived from 3-hourly measurements made at individual chambers in the bog and fen using a Quantum Cascade Laser Spectrometer (Aerodyne Research Inc.) connected to an automated chamber system (McCalley et al., 2014). Each chamber covered an area of 0.2 m^2 with a height of 15–75 cm depending on habitat vegetation and was closed for 5 min every 3 hours during CH_4 exchange measurements (McCalley et al., 2014). Water table depth measurements were taken in the bog and fen three to five times per week from June to October each year (McCalley et al., 2014). Peat samples were collected from 1 to 28 cm below the peat surface during the 2011 thawed season (15 June, 12 July, 16 August, and 16 October) at three locations adjacent to the bog and fen (Table S1). The relative abundance of methanogens was quantified in the peat samples using 16S rRNA gene amplicon sequencing to estimate the relative fractional contributions of AM and HM to total CH_4 production (McCalley et al., 2014; Mondav et al., 2014). The details of CH_4 exchange measurements and rRNA gene amplicon sequencing are described in McCalley et al. (2014) and Mondav et al. (2014).

2.3 GSWP3 Reanalysis Dataset

Global Soil Wetness Project Phase 3 (GSWP3) is an ongoing modeling activity that provides global gridded meteorological forcing (0.5° × 0.5° resolution) and investigates changes in energy, water, and carbon cycles throughout the 20th and 21st centuries (Kim, 2017). The GSWP3 reanalysis dataset is based on the 20th Century Reanalysis (Compo et al., 2011), and its spatial and temporal resolutions are finer than many other existing climate reanalysis datasets (Chang et al., 2019). A more detailed description of the GSWP can be found in Dirmeyer (2011) and van den Hurk et al. (2016).

The GSWP3 reanalysis dataset was reported to be biased cold and wet compared to the long-term ANS measurements at the Stordalen Mire, which could significantly limit model performance on thaw depth and carbon

cycling simulations (Chang et al., 2019). In this study, we extracted the 3-hourly GSWP3 meteorological conditions at the Stordalen Mire from 1901 to 2013, and bias-corrected the time series using the monthly mean biases calculated in this period based on the correction method described in Chang et al. (2019). The 3-hourly products of air temperature, precipitation, solar radiation, wind speed, and specific humidity were interpolated to hourly intervals with cubic spline interpolation to serve as the meteorological inputs used in our model (Figure S1).

2.4 Model Description

The ecosys model is a comprehensive biogeochemistry model that simulates ecosystem responses to diverse environmental conditions with explicit representations of microbial dynamics; soil carbon, nitrogen, and phosphorus biogeochemistry; plants; hydrology; and thermal dynamics. The aboveground processes are represented in multispecific multilayer plant canopies, and the belowground processes are represented in multiple soil layers with multiphase subsurface reactive transport. The ecosys model operates at variable time steps (~seconds to 1 hour) determined by convergence criteria, and it can be applied at patch scale (spatially homogenous one-dimensional; e.g., Mekonnen et al., 2018) and landscape scale (spatially variable two- or three-dimensional; e.g., Grant, Mekonnen, Riley, Arora, & Torn, 2017; Grant, Mekonnen, Riley, Wainwright, et al., 2017). A qualitative summary of the ecosys model is provided in the model description part of the supplementary material to this article, and detailed descriptions are available in the supplements of Grant (2013) and Grant, Mekonnen, Riley, Arora, & Torn (2017) Grant, Mekonnen, Riley, Wainwright, et al. (2017).

The rate at which soil organic matter in ecosys is hydrolyzed during decomposition is a first-order function of the decomposer biomass of all heterotrophic microbial populations (functional types) generated from energy yields of the oxidation-reduction reactions conducted by each population. Hydrolysis rates are regulated by soil temperature through an Arrhenius function (equation [4]) and by soil water content through its effect on aqueous microbial concentrations. Hydrolysis products are transferred to dissolved organic carbon (DOC) that is the substrate for respiration and uptake by microbial biomass. DOC utilization by aerobic and anaerobic respiration, fermentation, and consequent acetogenesis is estimated based on a Michaelis-Menten function of DOC concentration, and is regulated by soil temperature (equation 4) and oxygen availability. Fermentation products of DOC are partitioned among acetate (CH_3COOH), CO_2, and hydrogen (H_2) according to Brock and Madigan (1991):

$$\mathrm{DOC} \rightarrow 0.67\mathrm{CH_3COOH} + 0.33\mathrm{CO_2} + 0.11H_2 \quad (1)$$

The ecosys model represents AM and HM driven by biomasses of AM and HM functional types generated from AM and HM energy yields, with acetate, and

CO_2 and H_2 are being the substrates of these two CH_4 production pathways, respectively (Brock & Madigan, 1991):

$$CH_3COOH \rightarrow CO_2 + CH_4 \quad (2)$$

$$CO_2 + 4H_2 \rightarrow CH_4 + 2H_2O \quad (3)$$

The AM and HM modeled by ecosys are both regulated by (1) temperature stress according to an Arrhenius function,

$$S_T = \frac{exp(25.227 - H_a/RT_{soil})}{1 + \exp(([-ST_{soil}]/[RT_{soil}]). + \exp([ST_{soil} - H_{dh}]/[RT_{soil}])}; \quad (4)$$

(2) substrate stress based on Michaelis-Menten kinetics,

$$S_{S,AM} = V_{max,AM} \frac{[CH_3COOH]}{K_m + [CH_3COOH]}, \quad (5)$$

$$S_{S,HM} = V_{max,HM} \frac{[H_2]}{K_h + [H_2]} \frac{[CO_2]}{K_c + [CO_2]}; \quad (6)$$

and (3) moisture stress through an exponential function of soil water potential,

$$S_M = \exp(0.1\psi_s)). \quad (7)$$

The above-mentioned symbols represent temperature stress (S_T), substrate stress for AM ($S_{S,AM}$), substrate stress for HM ($S_{S,HM}$), moisture stress (S_M), energy of activation (H_a), energy of low temperature deactivation (H_{dl}), energy of high temperature deactivation (H_{dh}), change in entropy (S), gas constant (R), soil temperature (T_{soil}), maximum specific respiration rate for AM ($V_{max,AM}$), Michaeli-Menten constant for AM (K_m), maximum specific respiration rate for HM ($V_{max,HM}$), Michaelis-Menten constant for HM (H_2; K_h), Michaelis-Menten constant for HM (CO_2; K_c), and soil water potential (ψ_s), respectively. The definition of the variables and parameters used in equations 4–7 are summarized in Table S2, and the detailed equation sets are listed in Grant (2013). The amount of AM (HM) produced at each model time step is the product of potential AM (HM) production and substrate limitations. The amount of CH_4 produced at each model time step is the sum of AM production and HM production minus CH_4 oxidation.

The thaw depth (R^2 = 0.75–.90), CO_2 exchange (R^2 = 0.43–0.64), and CH_4 exchange (R^2 = 0.31–0.54) modeled by ecosys have been validated against multi-year (2002–2007) field records across the three landscape types at the Stordalen Mire, demonstrating that ecosys can represent the changing ecosystem responses observed along the permafrost thaw gradient (Chang et al., 2019). In addition, ecosys has been extensively tested against eddy covariance measurements in other permafrost-associated habitats (Grant, Mekonnen, Riley, Arora, & Torn, 2019; Grant, Mekonnen, & Riley, 2019; Grant, Mekonnen, Riley, Arora, & Torn, 2017; Grant, Mekonnen, Riley, Wainwright, et al., 2017; Grant & Roulet, 2002). All ecosys model structures are unchanged from those described in these earlier studies.

2.5 Experimental Design

To evaluate the effects of biogeophysical feedbacks on CH_4 dynamics, we conducted four sets of model experiments at the Stordalen Mire from 1901 to 2013. We used 10 canopy layers and 13 soil layers in each model experiment. The bias-corrected GSWP3 meteorological conditions from 1901 to 2001 were used for model initialization (i.e., spin-up, Chang et al., 2019), and those from 2002 to 2013 were used for analysis. The meteorological conditions for all the experiments were based on the bias-corrected climate forcing extracted from the GSWP3 reanalysis dataset (section 3.3). Based on field records, both moss and sedge were represented in bog simulations while only sedge was represented in fen simulations (Figure 1). Key soil property and vegetation parameters used in our simulation are listed in Tables S3 and S4, which represent the landscape differences between the bog and fen (section 3.1).

We first evaluated our model performance against bog and fen measured CH_4 emission magnitude and CH_4 production pathways (section 3.2), and we labeled these model scenarios “BOG” and “FEN”, respectively We then investigated the factors that could regulate CH_4 dynamics and thereby lead to the CH_4 cycling shifts observed along the permafrost thaw gradient. The primary differences between the bog and fen aboveground conditions are: (1) the presence of mosses in the bog and (2) the presence of inundation in the fen (Figure 1). The effects of moss cover on CH_4 dynamics were examined by reducing the amount of moss presented in experiment BOG through lowering initial moss planting density (labeled “BOG [moss−]”). The effects of inundation on CH_4 dynamics were examined by reducing surface water inundation in experiment FEN through lowering the external water table from 15 cm above the peat surface to 3 cm above the peat surface for years 2011–2013 (labeled “FEN [inundation−]”).

3 Results and Discussion

3.1 Biogeophysical Differences Among Model Experiments

Some of the key distinctions modeled in the 2011 thawed season are shown in Figure 2 as an example of the effects of different vegetation cover and inundation status in our four sets of experiments. For the two experiments conducted in the bog, lower initial moss planting density used in experiment BOG (moss−) results in lower moss Leaf Area Index (LAI) while preserving the amounts of sedge LAI and standing water (compared to experiment BOG; Figures 2a–2c). The LAI modeling processes are summarized in the Canopy carbon and nutrient cycling section in Supporting Information S3. For the two experiments conducted in the fen, lower external water table used in experiment FEN (inundation−) results in less standing water while preserving the sedge LAI (compared to experiment FEN (Figures 2a–2c). These differences in environmental conditions induced changes in soil moisture content and surface energy balance, resulting in different volumetric heat storage (energy stored in surface litter, water, and ice; Figure 2d) and soil

surface temperature (Figure 2e), even though all experiments were driven by the same meteorological forcing. We next focused on how these biogeophysical differences regulate CH_4 dynamics and contribute to the observed shifts in CH_4 production and emission along the permafrost thaw gradient at the Stordalen Mire.

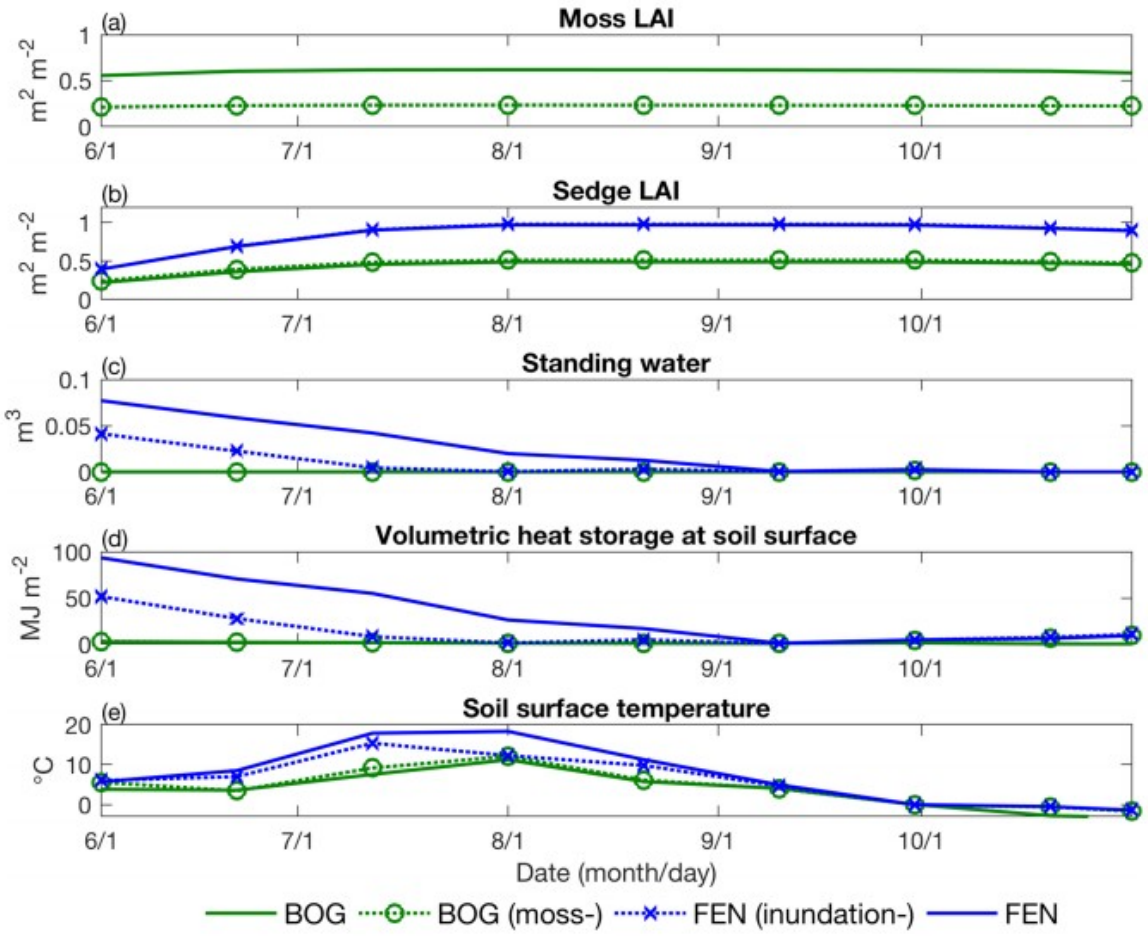

Figure 2. Modeled daily moss LAI (a), sedge LAI (b), volume of standing water per soil surface area (c), volumetric heat storage at soil surface (including the aboveground standing water; d), and soil surface temperature (e) for the four sets of experiments from June to October 2011. LAI = Leaf Area Index.

3.2 Model Evaluation

Modeled water table depths for experiments BOG and FEN generally capture the observed seasonal variations measured in the bog and fen from 2011 to 2013 (Figures 3a and 3c). During summer, the modeled water table depth fluctuates from −8 cm to −1 cm (negative implies below peat surface; −5.6 ± 1.2 cm; mean ± standard deviation) in experiment BOG, which is generally higher than measured in the bog (−8.5 ± 5.4 cm). Such biases were also reported in Chang et al. (2019) that applied the same model configuration for simulations conducted from 2003 to 2007. Chang et al. (2019) concluded that those biases were caused by the relatively simple topographic effects

represented in one-dimensional column simulations. For example, no excess water could be transported to neighboring gridcells to deepen its local water table depth, and vice versa. A multidimensional simulation that includes realistic topographic effects could help improve the representation of water table dynamics and reduce simulation errors. Modeled summertime water table depth is mostly above the peat surface in experiment FEN (7.1 ± 4.7 cm) and compares well to measured values (11.4 ± 3.0 cm). Modeled water table depths are less affected by the limitations of our one-dimensional column simulation in the fen, which could be related to the less variable water table depth measured above the peat surface.

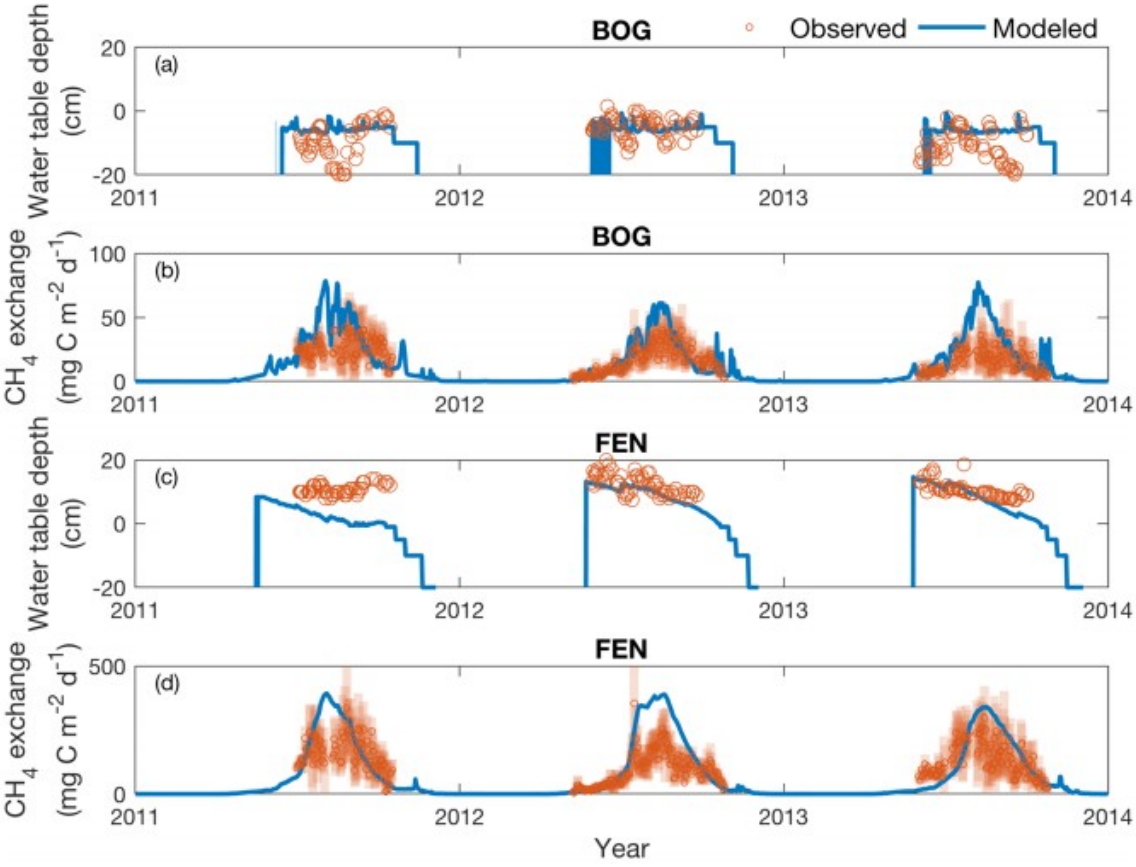

Figure 3. Modeled (solid lines) and measured (open circles) water table depths and daily CH_4 emissions at the bog and fen from 2011 to 2013. Shaded bars are the standard deviations of the daily CH_4 emissions measured across the automated chambers under each landscape type. CH_4 = methane.

Modeled and measured daily CH_4 exchanges correlated reasonably well in the bog (R^2 = 0.38) and fen (R^2 = 0.46) throughout the study period (Figures 3b and 3d). Both simulations and observations exhibit stronger CH_4 emissions during thawed seasons and peak emissions in late summer. The modeled daily mean CH_4 emissions are generally stronger than measured in the bog and fen, although many of the overestimations (54% in the bog and 52% in the fen) are within the measurement variability across different

automated chambers in the same landscape type. In addition to model structural uncertainty, the differences between the modeled and measured CH_4 emissions could result from the lack of micrometeorological forcing and quantitative vegetation description at each automated chamber. Future model improvement requires better constraints from additional biometeorological measurements to address the high spatial heterogeneity presented in high-latitude peatlands (Malhotra & Roulet, 2015; Olefeldt et al., 2013). Some episodic CH_4 emission pulses (Mastepanov et al., 2008) were modeled during shoulder seasons in the bog and fen, although the magnitudes were relatively lower than the modeled summertime emissions. Modeled seasonal cycles of microbial CH_4 production rates were aligned with the modeled CH_4 exchanges in the bog and fen, and their variation patterns were consistent from 2011 to 2013 (not shown). For conciseness, results modeled in 2011 were analyzed to investigate the seasonal dynamics of CH_4 production; similar results were found in 2012 and 2013.

Modeled HM fractions (i.e., HM/[HM + AM]) are consistent with measurements of the relative abundances of HM and AM methanogenic lineages reported in McCalley et al. (2014) during the 2011 thawed season (Figure 4). Note that the measured HM fractions reflect microbial community composition, which may not necessarily represent the ratio of HM to total CH_4 production estimated by the model. Both modeled and measured HM fractions exhibit significant vertical variability that complicates quantitative evaluation of model performance, although both metrics suggest decreased HM fraction from the bog to the fen. Additionally, such strong vertical variability in HM fraction demonstrates that single point measurements of this metric are unlikely to produce a realistic representation of the underlying complex dynamics. Both the modeled and measured HM fractions suggest that HM is the primary (greater than 50%) CH_4 production pathway in the bog, and the modeled HM fraction exhibits weak seasonal variability when CH_4 production rate is relatively strong (July to August; Figure 4a). Conversely, the HM fraction modeled in the fen decreases significantly with increased CH_4 production rate from July to August, exhibiting stronger seasonal variability in CH_4 production rate and pathway (Figure 4b). The contrasting temporal trends between HM fraction and CH_4 production rates modeled in the fen indicate that the dominant CH_4 production pathway in a given ecosystem may vary with time, suggesting that such process should not be statically prescribed in biogeochemical models. Therefore, it appears important for models to explicitly represent AM and HM cycling to reduce model structural uncertainty in simulating CH_4 production, although it is not yet clear if such efforts will improve CH_4 emission estimates at ecosystem scales (Deng et al., 2014, 2017).

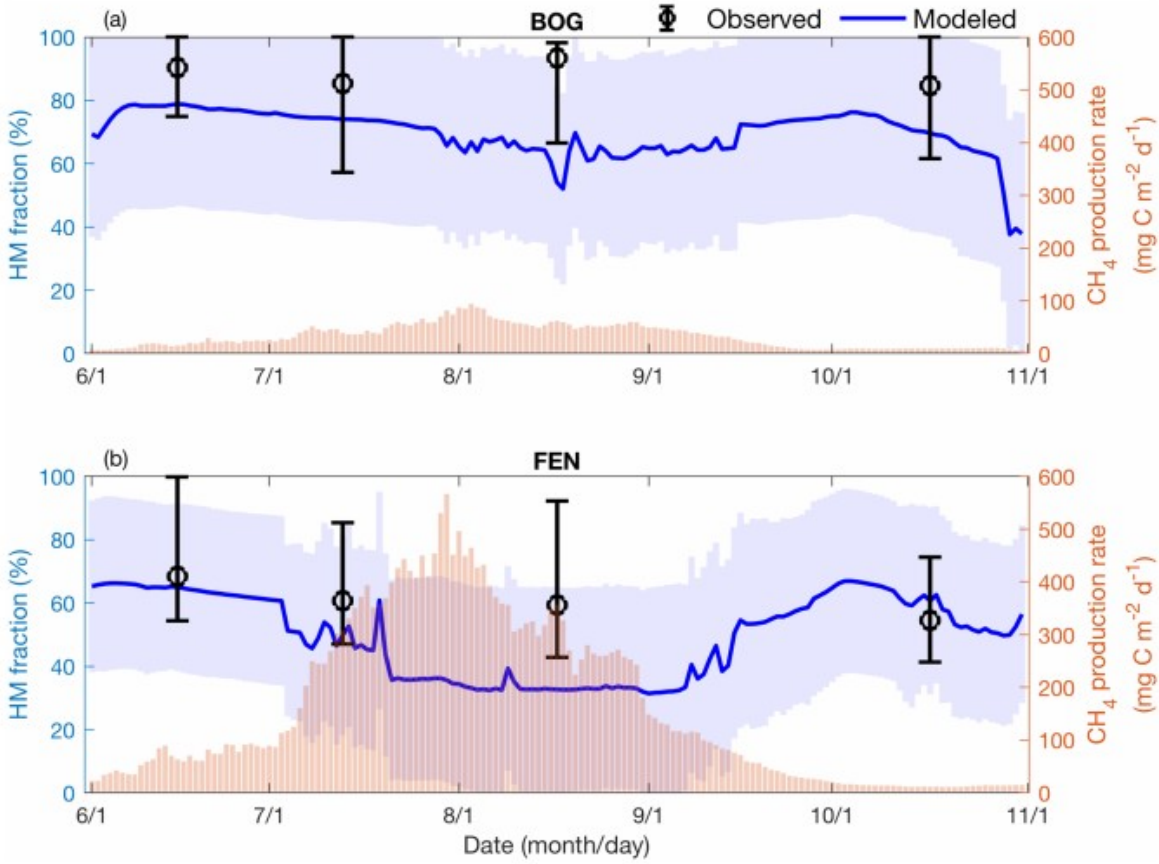

Figure 4. Modeled fractional contribution of HM to total CH_4 production (blue lines; left *y*-axis) and daily CH_4 production (red bars; right *y*-axis) in the bog (a) and fen (b) from June to October 2011. Shaded area is the vertical variability of modeled HM fraction along the soil profile. Black open circles and error bars are the observed means and ranges, respectively, of the relative abundance of HM to total methanogenic lineages derived from McCalley et al. (2014). CH_4 = methane; HM = hydrogenotrophic methanogenesis.

3.3 CH_4 Production Dynamics Dependence on Soil Temperature

The fact that ecosys is able to reasonably simulate the observed differences between the bog and fen (section 4.2) indicates that the modeled CH_4 dynamics are attributed to differences in soil, hydrology, and vegetation conditions, since experiments BOG and FEN only differ in those biogeophysical parameters (Tables S3 and S4). The higher pH values and lower peat carbon to nitrogen (CN) ratios measured in the fen were hypothesized to underlie the CH_4 production differences between the bog and fen (Hodgkins et al., 2014). The modeled CH_4 production rates and pathways were not very sensitive to shifts in pH values and peat CN ratios imposed on our sensitivity tests (not shown), suggesting that our model may not be comprehensive enough to resolve processes driven by changing organic matter chemistry. Instead, our results indicate that the modeled CH_4 production differences between the bog and fen were primarily caused by soil temperature differences that resulted from the different vegetation cover and inundation status along the permafrost thaw gradient (Figures 5a and

5d). We found that (1) the presence of moss increases latent heat flux (greater evapotranspiration) at the expense of sensible heat flux, consistent with many high-latitude observations (Brown et al., 2010; Heijmans et al., 2004; J. Kim & Verma, 1996); and (2) the presence of surface water inundation increases heat storage at and above the soil surface (Figure 2d) that provides additional energy to warm the underlying soil. We also found that not all changes in vegetation substantially influence modeled CH_4 production. For example, changes in the amount of sedge have limited effects on the CH_4 production rate and pathway modeled in a series of sensitivity tests (not shown), and their effects are too small to explain observed shifts in the primary CH_4 production pathway between the bog and fen.

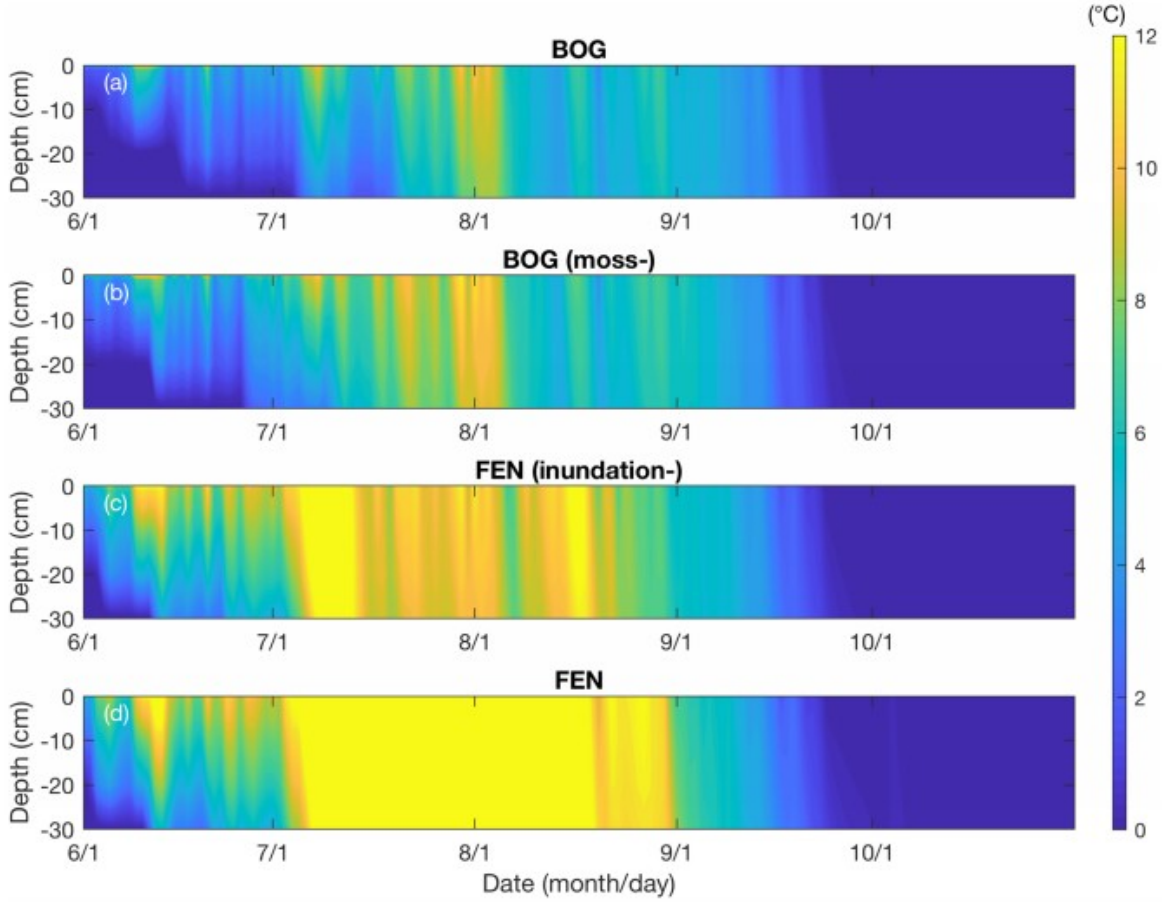

Figure 5. Modeled June to October 2011 daily soil temperature profiles in experiments BOG (a), BOG (moss−; b), FEN (inundation−; c), and FEN (d).

The modeled fen soil temperatures are significantly warmer than in the bog, due to the absence of moss and the presence of surface water inundation in experiment FEN (Figures 5a and 5d). Also, the modeled soil temperature becomes cooler with increased moss cover in the bog (Figures 5a and 5b), and reduced surface water inundation in the fen (Figures 5c and 5d). The soil

temperature samples measured in the 2011 thawed season support our simulation results; those measurements show that the fen soil was warmer than the bog at 13 cm by 9.1, 6.1, and 2.3 °C in June, July, and Aug, respectively. The monthly mean soil temperature profiles reported in Lupascu et al. (2012) also suggest that the fen soil is systematically warmer than the bog at the Stordalen Mire (Figure S2).

Changes in soil temperature led by different vegetation cover and inundation status prescribed in our four sets of model experiments (Figure 5) caused different CH_4 production rates (Figure 6). The modeled CH_4 production rate exhibits strong temporal variability and vertical and landscape-type heterogeneity, and it generally increases with warmer soil temperatures resulting from seasonality, vegetation composition (Figures 6a and 6b), and surface water inundation (Figures 6c and 6d). Such temperature dependence is associated with the Arrhenius equation used in ecosys that stimulates higher DOC respiration that increases AM and HM substrates for stronger CH_4 production (equations [1]–[4]), which is consistent with the laboratory incubation results shown in Lupascu et al. (2012). In addition, the modeled CH_4 production is largely confined within the top 20 cm of soil where microbial biomass responsible for AM and HM is mostly concentrated (not shown). The modeled CH_4 production profiles are consistent with laboratory incubations that record decreased CH_4 production rates with increasing soil depth (Lupascu et al., 2012). Such variations in CH_4 production profiles highlight the need to realistically represent complex CH_4 dynamics; however, there are currently very limited measurements to validate the cause of spatial heterogeneity modeled along the soil vertical profile. We therefore focus our discussion below on the landscape-type heterogeneity modeled along the permafrost thaw gradient, where more measurements are currently available, to investigate the cause of spatial and temporal variations in CH_4 production (section 4.4).

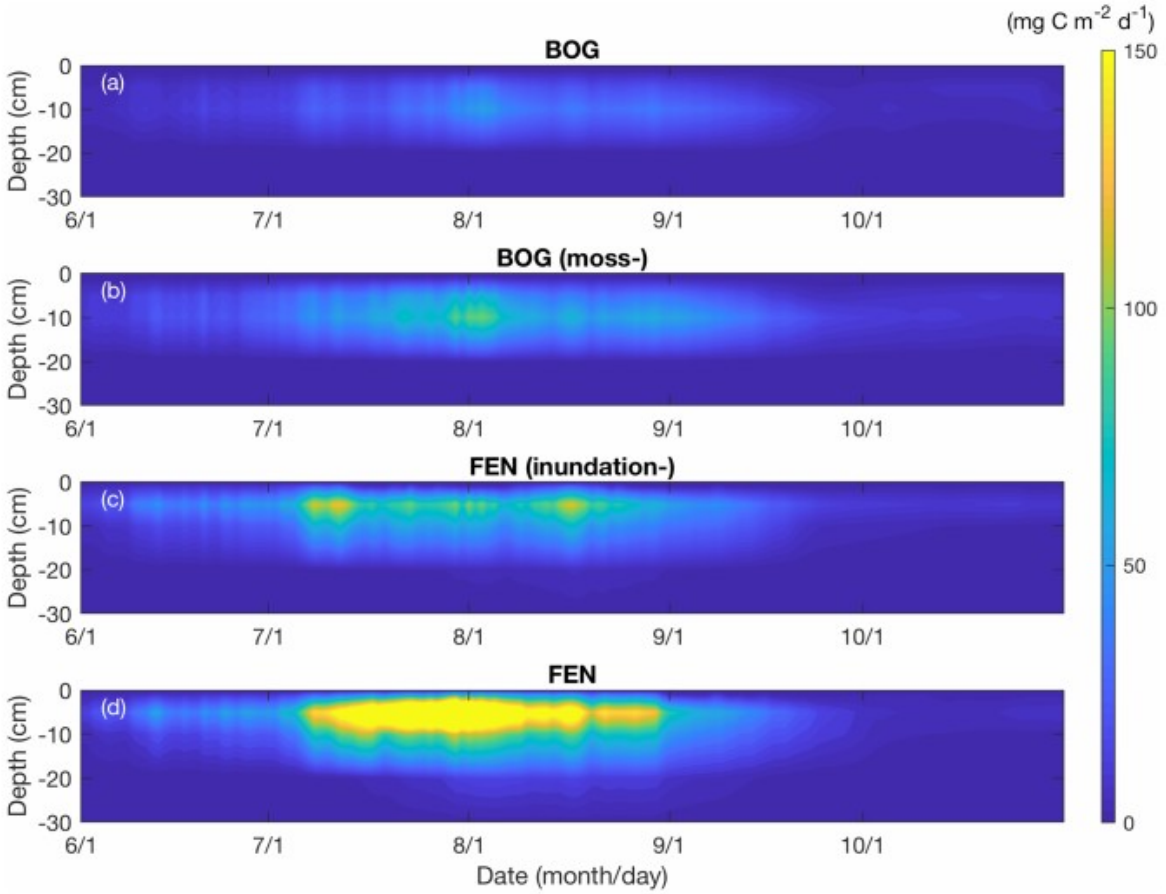

Figure 6. Modeled daily CH_4 production (HM + AM) profile in experiments BOG (a), BOG (moss-; b), FEN (inundation-; c), and FEN (d) from June to October 2011. AM = acetoclastic methanogenesis; HM = hydrogenotrophic methanogenesis.

Modeled CH_4 oxidation rates exhibit similar spatial heterogeneity along the permafrost thaw gradient and along the soil vertical profile as the modeled CH_4 production rate, with a much weaker magnitude (Figure 7). In terms of temporal variability, the modeled peak CH_4 oxidation rate generally lags behind the modeled peak CH_4 production rate, and the modeled shoulder season CH_4 oxidation rate is stronger than that during midsummer. Our results indicate strong seasonality in CH_4 oxidation to CH_4 production ratio, and less than 5% of the modeled CH_4 production is oxidized to CO_2 during the peak CH_4 emission period (i.e., July to August; Figure S3). The limited effects of CH_4 oxidation modeled in our four sets of experiments suggests that CH_4 oxidation is unlikely to determine the observed shifts in CH_4 emission rate along the permafrost thaw gradient, which is consistent with isotopic validations (Hodgkins et al., 2014; McCalley et al., 2014).

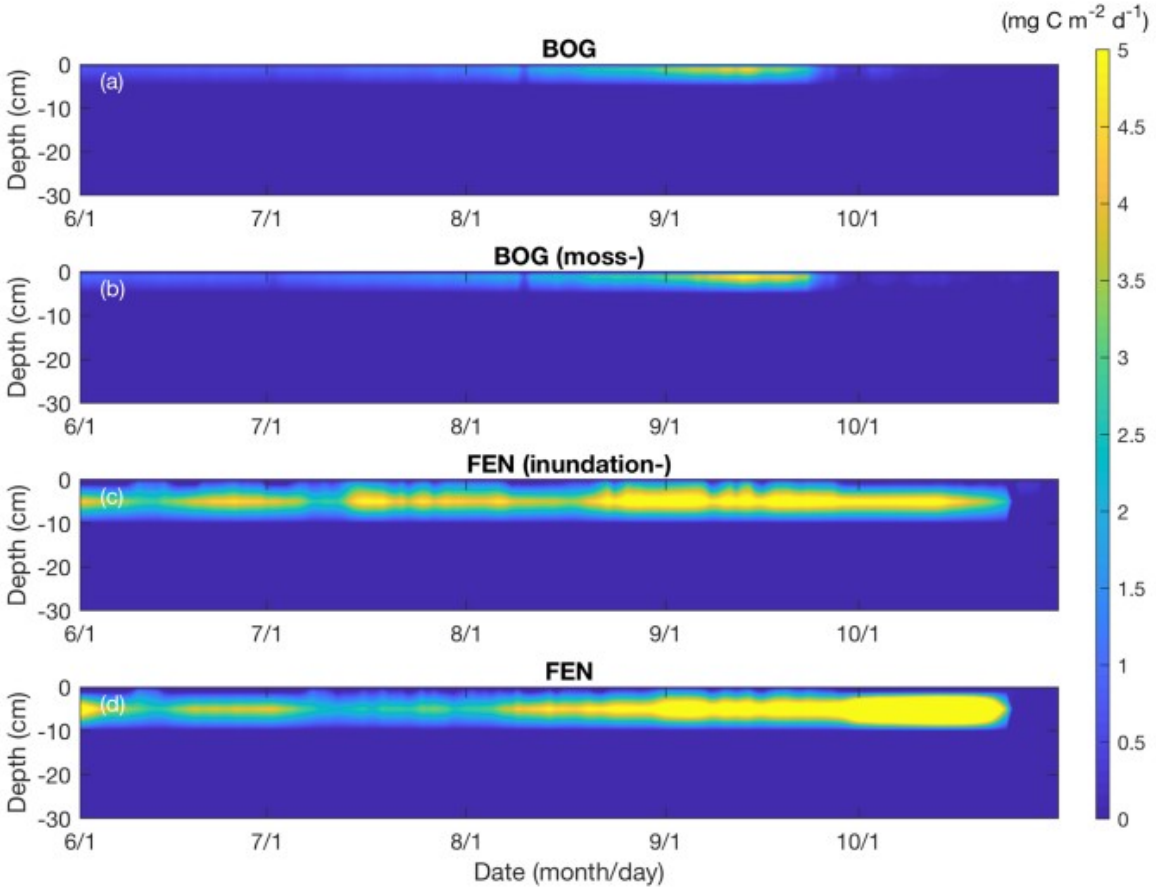

Figure 7. Modeled daily CH_4 oxidation profile in experiments BOG (a), BOG (moss-; b), FEN (inundation-; c), and FEN (d) from June to October 2011.

3.4 Factors Regulating CH_4 Dynamics

The AM and HM CH_4 production rates both increase along the permafrost thaw gradient, as the total amount of CH_4 (AM + HM) produced in the 2011 thawed season increases with increasing mean soil temperature (Figure 8b). Our results show that the amount of CH_4 produced in the fen is 8.1, 3.7, and 5.0 times greater than the bog for AM, HM, and total CH_4 production, respectively. The amount of CH_4 produced by AM increases more rapidly than HM across the permafrost thaw gradient, which decreases the fractional contribution of HM to total CH_4 production from 71% in the bog to 53% in the fen (Figure 8a). The increase in AM modeled with greater inundation in the fen could be caused by reduced competition for acetate modeled between aerobic heterotrophs and acetotrophic methanogens under more anoxic conditions. Such shifts in CH_4 production pathways were observed in McCalley et al. (2014), who hypothesized that thawing permafrost could induce changes in microbial community composition that regulate CH_4 dynamics. Since ecosys reasonably depicts the observed shifts in CH_4 production pathways without prescribing microbial community composition,

its model structure could be a compromise that broadly links CH_4 dynamics between microbial and ecosystem scales for process-based modeling.

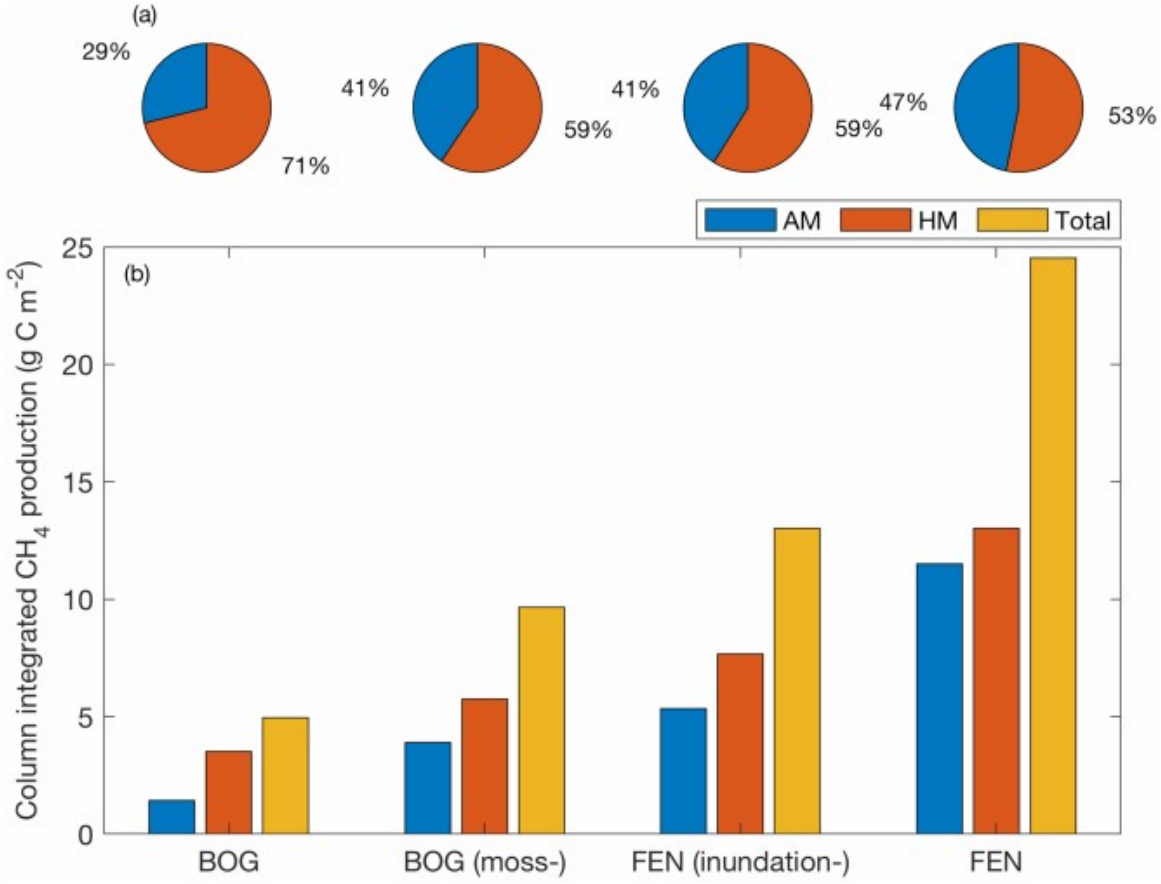

Figure 8. Modeled mean AM and HM partitioning aggregated from June to October 2011 (a). The modeled amounts of AM, HM, and total (AM + HM) CH_4 production cumulated from June to October 2011 (b). Modeled AM fraction and CH_4 production rates both increase from the bog to the fen. AM = acetoclastic methanogenesis; HM = hydrogenotrophic methanogenesis.

We disaggregate the factors determining modeled AM and HM production rates along the permafrost thaw gradient to diagnose the cause of observed shifts in CH_4 emission magnitude and CH_4 production pathways. We calculated the apparent CH_4 production stress based on the weighted average between CH_4 production stress factors (equations.[4]–[7]) and the corresponding AM and HM microbial biomass in the top 20 cm of soil (where most CH_4 was produced, Figure 6) to represent the individual stress effects on AM and HM production. The results show that the seasonal variability of temperature stress and substrate stress is higher in the fen than the bog, and the moisture stress has very small effects on CH_4 production in the bog and fen (Figure 9). The temperature stress remains relatively strong in the bog throughout the 2011 thawed season, and inhibits AM and HM growth. In contrast, the fen temperature stress is effectively relieved by the warmer soil temperatures modeled from July to August (Figure 5d), which aligns with the

stronger CH_4 production rates during this period (Figure 6d). Noticeably, the bog substrate stress for AM is stronger (i.e., more stressed) than HM, and both are weaker (i.e., less stressed) than the temperature stress (Figure 9a). The AM substrate stress becomes weaker than HM when the temperature stress becomes weaker in the fen (Figure 9b). Therefore, our results suggest that changes in temperature stress indirectly affect AM and HM through altering substrate stress via asymmetric fractionation of DOC (equation [1]) whose magnitude is responding to soil temperature (equation [4]).

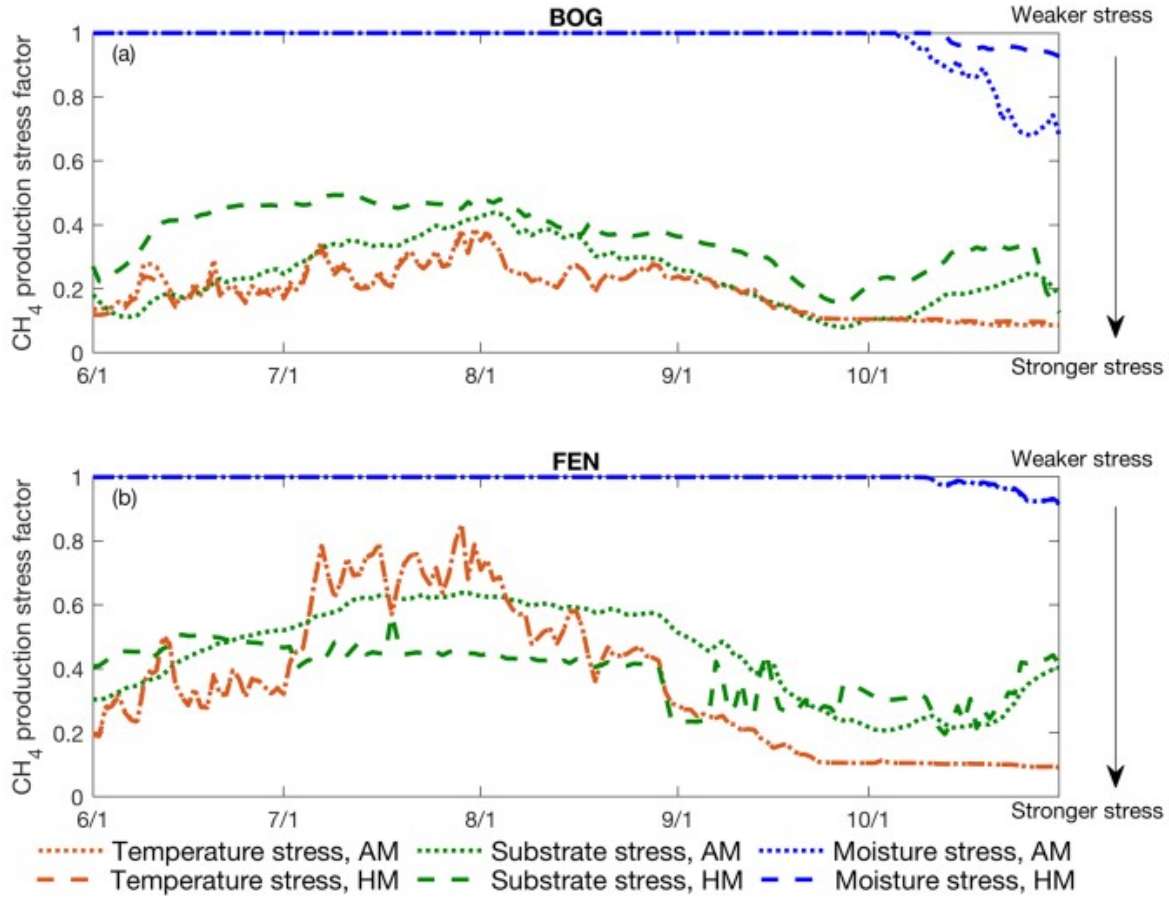

Figure 9. Daily CH_4 production stress factors modeled in the bog (a) and fen (b) from June to October 2011. Higher values of the CH_4 production stress factor represent weaker CH_4 production stress. AM = acetoclastic methanogenesis; HM = hydrogenotrophic methanogenesis.

The monthly mean CH_4 production stress factors show that the temperature stress and substrate stress for AM and HM are both significantly stronger (more stressed) in the bog than the fen in July 2011 (Figure 10), and most of the 2011 thawed season (Figure S4). Our results indicate that the stronger temperature stress, not the stronger substrate stress, is responsible for the weaker CH_4 production modeled in the bog. In addition to the stronger temperature stress directly inhibiting AM and HM, lower soil temperatures reduce DOC respiration and thereby constrain AM and HM substrates

(section 3.4). The rate of increase in substrate availability is higher for AM than HM with enhanced DOC respiration induced by weaker temperature stress because the acetate production rate is higher than the hydrogen production rate (equation 1). Consequently, AM substrate rises relatively more with increased soil temperature than does HM substrate, and this temperature stress-induced asymmetric increase in substrate availability affects AM and HM rates. Our results show that the proximal and distal limiting factors determining the primary CH_4 production pathway are substrate stress and soil temperature, respectively (Figure 10). For example, the weaker substrate stress for HM results in higher HM fraction in the cooler bog soil while the corresponding temperature stress is relatively strong for both AM and HM (Figure 10). A similar relationship between CH_4 production stress and HM fraction exists in the relatively cool fen soil in June (Figure S4a); however, the substrate stress for HM becomes stronger than AM with reduced temperature stress as the fen soil becomes warmer in July (Figure 10). The increased substrate stress for HM and decreased substrate stress for AM decrease the HM fraction when the fen soil is relatively warm leading to a greater seasonal variability of modeled fen HM fraction (Figure 4b).

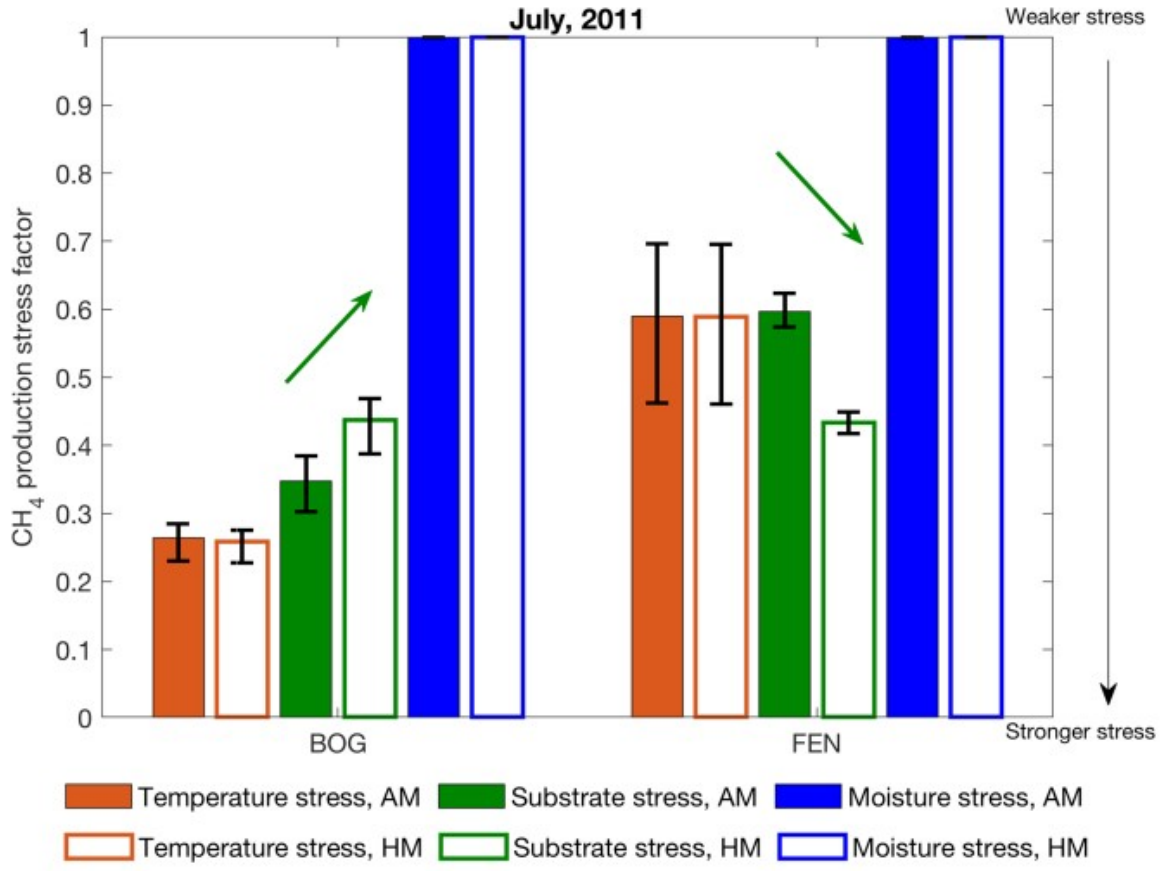

Figure 10. The CH_4 production stress factors modeled in the bog and fen in July 2011. Bars and error bars are the daily means and standard deviations, respectively. Lower values of the CH_4 production stress factor represent weaker CH_4 production stress. Green arrows indicate the relative strength of AM and HM substrate stress modeled in the bog and fen during this period. AM = acetoclastic methanogenesis; HM = hydrogenotrophic methanogenesis.

Overall, soil temperature shifts driven by changing biogeophysical conditions along the permafrost thaw gradient regulate CH_4 production rates through changing temperature stress and also affect the HM fraction through temperature-induced changes in substrate stress. The projected warming and wetting trends in high-latitude regions (Bintanja & Andry, 2017; Collins et al., 2013) could thus enhance peatland CH_4 production rates with higher AM fraction through reductions of temperature stress and substrate stress for AM.

In terms of model development, our results suggest that a model that incorporates dynamic interactions among biogeophysics, biogeochemistry, and microbial dynamics could be comprehensive enough to reasonably represent the shifts in CH_4 dynamics observed at ecosystem scales. Differences in ecosystem characteristics can lead to different soil thermal and hydrological conditions thereby altering biogeochemical responses under the same climate forcing. In particular, the modeled substrate stress responds differently to changes in soil temperature across landscape types,

so it may be necessary to explicitly represent AM and HM pathways to reduce model structural uncertainty in CH_4 production. Additionally, the representation of microbial responses to changing environmental conditions plays an important role in regulating CH_4 dynamics, and such functional dependency should be incorporated into process-based models at the ecosystem scale. Improvements in biogeophysical process parameterization and advances in quality-controlled field measurements could reduce the uncertainty in modeled soil hydrology and thereby CH_4 cycling driven by incomplete ecosystem structural and functional representation. Regional- and global-scale models should account for shifting CH_4 dynamics driven by fine-scale spatial heterogeneity, although a proper parameterization for scaling up such fine scale processes remains challenging.

4 Conclusion

Recent studies have found that permafrost thaw induces changes in microbial communities, vegetation, and water table depth that could enhance CH_4 emissions with increased AM (Hodgkins et al., 2014; McCalley et al., 2014; Mondav et al., 2014; Woodcroft et al., 2018). We successfully modeled measured shifts in CH_4 emissions and CH_4 production pathways along a permafrost thaw gradient at our northern Sweden Stordalen Mire site using the ecosystem-scale biogeochemical model ecosys. Our results show that changes in biogeophysical conditions can induce significant changes in soil temperature that lead to shifts in CH_4 production rates and pathways under different permafrost thaw stages (i.e., bog and fen). The strong soil temperature dependence demonstrates that models can represent complex CH_4 dynamics without prescribing microbial community composition, although such model structure may not be comprehensive enough to resolve processes driven by changing organic matter chemistry. CH_4 oxidation is a small factor in this system during the peak CH_4 emission period (July to August), and is unlikely to cause the CH_4 dynamics shifts observed at our study sites. Moreover, changes in soil temperature indirectly regulate substrate availability for AM and HM, which controls the relative importance of the two CH_4 production pathways. Our results show that the modeled fractional contribution of HM to total CH_4 production was 71% and 53% in the bog and fen, respectively, over the 2011 thawed season, due to the warmer fen soil induced by surface water inundation and reduced moss cover. Our results show that a proper parameterization for microbial dynamics is necessary to predict shifting CH_4 cycling under a changing climate, and it may be important to explicitly represent AM and HM pathways to reduce model structural uncertainty of CH_4 production. Our findings suggest that increased soil temperature under projected high-latitude warming and wetting trends (Bintanja & Andry, 2017; Collins et al., 2013) could enhance peatland CH_4 production with elevated AM fraction, even without further permafrost degradation. The magnitude of high-latitude peatland CH_4 emissions could increase with such increases in CH_4 production due to the relatively weak CH_4 oxidation rate modeled in this system, which reinforces

the need for an appropriate metric to quantify the potential strong CH_4 radiative forcing (Neubauer & Megonigal, 2015) in the climate system.

Acknowledgments

This study was funded by the Genomic Science Program of the United States Department of Energy Office of Biological and Environmental Research under the IsoGenie project, grant DE-SC0016440. Part of this work was performed at Lawrence Berkeley National Laboratory under contract DE-AC02-05CH11231. We thank the ANS of the Swedish Polar Research Secretariat for providing the meteorological data. We are furthermore thankful to the two anonymous reviewers who provided constructive comments that improved the manuscript. The data presented in this study are available at the IsoGenie Database (https://isogenie-db.asc.ohio-state.edu/datasources\T1\textbackslash#modeling).

References

Bäckstrand, K., Crill, P. M., Jackowicz-Korczyñski, M., Mastepanov, M., Christensen, T. R., & Bastviken, D. (2010). Annual carbon gas budget for a subarctic peatland, Northern Sweden. *Biogeosciences*, 7(1), 95– 108. https://doi.org/10.5194/bg-7-95-2010

Bäckstrand, K., Crill, P. M., Mastepanov, M., Christensen, T. R., & Bastviken, D. (2008a). Non-methane volatile organic compound flux from a subarctic mire in Northern Sweden. *Tellus Series B: Chemical and Physical Meteorology*. https://doi.org/10.1111/j.1600-0889.2007.00331.x

Bäckstrand, K., Crill, P. M., Mastepanov, M., Christensen, T. R., & Bastviken, D. (2008b). Total hydrocarbon flux dynamics at a subarctic mire in northern Sweden. *Journal of Geophysical Research – Biogeosciences*. https://doi.org/10.1029/2008JG000703

Bintanja, R., & Andry, O. (2017). Towards a rain-dominated Arctic. *Nature Climate Change*, 7(4), 263– 267. https://doi.org/10.1038/nclimate3240

Brock, T. D., & Madigan, M. T. (1991). *Biology of microorganisms* (6th ed.). NJ: Prentice Hall.

Brown, S. M., Petrone, R. M., Mendoza, C., & Devito, K. J. (2010). Surface vegetation controls on evapotranspiration from a sub-humid Western Boreal Plain wetland. *Hydrological Processes*, 24(8), 1072– 1085. https://doi.org/10.1002/hyp.7569

Callaghan, T. V., Bergholm, F., Christensen, T. R., Jonasson, C., Kokfelt, U., & Johansson, M. (2010). A new climate era in the sub-Arctic: Accelerating climate changes and multiple impacts. *Geophysical Research Letters*, L14705. https://doi.org/10.1029/2009GL042064

Chang, K.-Y., Riley, W. J., Crill, P. M., Grant, R. F., Rich, V. I., & Saleska, S. R. (2019). Large carbon cycle sensitivities to climate across a permafrost thaw

gradient in subarctic Sweden. *The Cryosphere*, 13(2), 647– 663. https://doi.org/10.5194/tc-13-647-2019

Chanton, J. (2005). The effect of gas transport on the isotope signature of methane in wetlands. *Organic Geochemistry*, 36, 753– 768. https://doi.org/10.1016/j.orggeochem.2004.10.007

Christensen, T. R., Johansson, T., Åkerman, H. J., Mastepanov, M., Malmer, N., Friborg, T., Crill, P., & Svensson, B. H. (2004). Thawing sub-arctic permafrost: Effects on vegetation and methane emissions. *Geophysical Research Letters*, 31, L04501. https://doi.org/10.1029/2003GL018680

Collins, M., Knutti, R., Arblaster, J., Dufresne, J.-L., Fichefet, T., Friedlingstein, P., Gao, X., Gutowski, W. J., Johns, T., Krinner, G., Shongwe, M., Tebaldi, C., Weaver, A. J., & Wehner, M. (2013). Long-term climate change: Projections, commitments and irreversibility. In V. Bex, P. M. Midgley, T. F. Stocker, D. Qin, G.-K. Plattner, M. Tignor, S. K. Allen, J. Boschung, A. Nauels, & Y. Xia (Eds.), *Climate Change 2013 the Physical Science Basis: Working Group I Contribution to the Fifth Assessment Report of the Intergovernmental Panel on Climate Change* (pp. 1029– 1136). Cambridge, UK and New York: Cambridge University Press. https://doi.org/10.1017/CBO9781107415324.024

Compo, G. P., Whitaker, J. S., Sardeshmukh, P. D., Matsui, N., Allan, R. J., Yin, X., Gleason, B. E., Vose, R. S., Rutledge, G., Bessemoulin, P., Brönnimann, S., Brunet, M., Crouthamel, R. I., Grant, A. N., Groisman, P. Y., Jones, P. D., Kruk, M. C., Kruger, A. C., Marshall, G. J., Maugeri, M., Mok, H. Y., Nordli, Ø., Ross, T. F., Trigo, R. M., Wang, X. L., Woodruff, S. D., & Worley, S. J. (2011). The Twentieth Century Reanalysis Project. *Quarterly Journal of the Royal Meteorological Society*, 137(654), 1– 28. https://doi.org/10.1002/qj.776

Deng, J., Li, C., Frolking, S., Zhang, Y., Bäckstrand, K., & Crill, P. (2014). Assessing effects of permafrost thaw on C fluxes based on multiyear modeling across a permafrost thaw gradient at Stordalen, Sweden. *Biogeosciences*, 11(17), 4753– 4770. https://doi.org/10.5194/bg-11-4753-2014

Deng, J., McCalley, C. K., Frolking, S., Chanton, J., Crill, P., Varner, R., Tyson, G., Rich, V., Hines, M., Saleska, S. R., & Li, C. (2017). Adding stable carbon isotopes improves model representation of the role of microbial communities in peatland methane cycling. *Journal of Advances in Modeling Earth Systems*, 9, 1412– 1430. https://doi.org/10.1002/2016MS000817

Dirmeyer, P. A. (2011). A history and review of the Global Soil Wetness Project (GSWP). *Journal of Hydrometeorology*, 12(5), 729– 749. https://doi.org/10.1175/JHM-D-10-05010.1

Fournier, G. P., & Gogarten, J. P. (2008). Evolution of acetoclastic methanogenesis in Methanosarcina via horizontal gene transfer from

cellulolytic Clostridia. *Journal of Bacteriology*. https://doi.org/10.1128/JB.01382-07

Grant, R. F. (2013). Modelling changes in nitrogen cycling to sustain increases in forest productivity under elevated atmospheric CO2 and contrasting site conditions. *Biogeosciences*, 10(11), 7703– 7721. https://doi.org/10.5194/bg-10-7703-2013

Grant, R. F., Mekonnen, Z. A., & Riley, W. J. (2019). Modeling climate change impacts on an Arctic polygonal tundra: 1. Rates of permafrost thaw depend on changes in vegetation and drainage. *Journal of Geophysical Research: Biogeosciences*, 124, 1308– 1322. https://doi.org/10.1029/2018JG004644

Grant, R. F., Mekonnen, Z. A., Riley, W. J., Arora, B., & Torn, M. S. (2017). Mathematical modelling of Arctic polygonal tundra with ecosys: 2. Microtopography determines how CO2 and CH4 exchange responds to changes in temperature and precipitation. *Journal of Geophysical Research: Biogeosciences*, 122, 3174– 3187. https://doi.org/10.1002/2017JG004037

Grant, R. F., Mekonnen, Z. A., Riley, W. J., Arora, B., & Torn, M. S. (2019). Modeling climate change impacts on an Arctic polygonal tundra: 2. Changes in CO_2 and CH_4 exchange depend on rates of permafrost thaw as affected by changes in vegetation and drainage. *Journal of Geophysical Research: Biogeosciences*, 124, 1323– 1341. https://doi.org/10.1029/2018JG004645

Grant, R. F., Mekonnen, Z. A., Riley, W. J., Wainwright, H. M., Graham, D., & Torn, M. S. (2017). Mathematical modelling of arctic polygonal tundra with ecosys: 1. Microtopography determines how active layer depths respond to changes in temperature and precipitation. *Journal of Geophysical Research: Biogeosciences*, 122, 3161– 3173. https://doi.org/10.1002/2017JG004035

Grant, R. F., & Roulet, N. T. (2002). Methane efflux from boreal wetlands: Theory and testing of the ecosystem model Ecosys with chamber and tower flux measurements. *Global Biogeochemical Cycles*, 16(4), 1054. https://doi.org/10.1029/2001GB001702

Heijmans, M. M. P. D., Arp, W. J., & Chapin, F. S. III (2004). Controls on moss evaporation in a boreal black spruce forest. *Global Biogeochemical Cycles*, 18, GB2004. https://doi.org/10.1029/2003GB002128

Hines, M. E., Duddleston, K. N., Rooney-Varga, J. N., Fields, D., & Chanton, J. P. (2008). Uncoupling of acetate degradation from methane formation in Alaskan wetlands: Connections to vegetation distribution. *Global Biogeochemical Cycles*, 22, GB2017. https://doi.org/10.1029/2006GB002903

Hodgkins, S. B., Tfaily, M. M., McCalley, C. K., Logan, T. A., Crill, P. M., Saleska, S. R., Rich, V. I., & Chanton, J. P. (2014). Changes in peat chemistry associated with permafrost thaw increase greenhouse gas production. *Proceedings of the National Academy of Sciences*, 111(16), 5819– 5824. https://doi.org/10.1073/pnas.1314641111

Hornibrook, E. R. C., Longstaffe, F. J., & Fyfe, W. S. (1997). Spatial distribution of microbial methane production pathways in temperate zone wetland soils: Stable carbon and hydrogen isotope evidence. *Geochimica et Cosmochimica Acta*, 61(4), 745– 753. https://doi.org/10.1016/S0016-7037(96)00368-7

Hugelius, G., Strauss, J., Zubrzycki, S., Harden, J. W., Schuur, E. A. G., Ping, C. L., Schirrmeister, L., Grosse, G., Michaelson, G. J., Koven, C. D., O'Donnell, J. A., Elberling, B., Mishra, U., Camill, P., Yu, Z., Palmtag, J., & Kuhry, P. (2014). Estimated stocks of circumpolar permafrost carbon with quantified uncertainty ranges and identified data gaps. *Biogeosciences*, 11(23), 6573– 6593. https://doi.org/10.5194/bg-11-6573-2014

Johansson, T., Malmer, N., Crill, P. M., Friborg, T., Åkerman, J. H., Mastepanov, M., & Christensen, T. R. (2006). Decadal vegetation changes in a northern peatland, greenhouse gas fluxes and net radiative forcing. *Global Change Biology*, 12(12), 2352– 2369. https://doi.org/10.1111/j.1365-2486.2006.01267.x

Kim, H. (2017). Global Soil Wetness Project Phase 3 atmospheric boundary conditions (Experiment 1) [Data set]. *Data Integration and Analysis System (DIAS)*. https://doi.org/https://doi.org/10.20783/DIAS.501

Kim, J., & Verma, S. B. (1996). Surface exchange of water vapour between an open sphagnum fen and the atmosphere. *Boundary-Layer Meteorology*, 79(3), 243– 264. https://doi.org/10.1007/bf00119440

Knoblauch, C., Beer, C., Liebner, S., Grigoriev, M. N., & Pfeiffer, E. M. (2018). Methane production as key to the greenhouse gas budget of thawing permafrost. *Nature Climate Change*, 8(4), 309– 312. https://doi.org/10.1038/s41558-018-0095-z

Kokfelt, U., Reuss, N., Struyf, E., Sonesson, M., Rundgren, M., Skog, G., Rosén, P., & Hammarlund, D. (2010). Wetland development, permafrost history and nutrient cycling inferred from late Holocene peat and lake sediment records in subarctic Sweden. *Journal of Paleolimnology*, 44(1), 327– 342. https://doi.org/10.1007/s10933-010-9406-8

Kotsyurbenko, O. R., Friedrich, M. W., Simankova, M. V., Nozhevnikova, A. N., Golyshin, P. N., Timmis, K. N., & Conrad, R. (2007). Shift from acetoclastic to H2-dependent methanogenesis in a West Siberian peat bog at Low pH values and isolation of an acidophilic *Methanobacterium* strain. *Applied and Environmental Microbiology*, 73(7), 2344– 2348. https://doi.org/10.1128/AEM.02413-06

Koven, C. D., Ringeval, B., Friedlingstein, P., Ciais, P., Cadule, P., Khvorostyanov, D., Krinner, G., & Tarnocai, C. (2011). Permafrost carbon-climate feedbacks accelerate global warming. *Proceedings of the National Academy of Sciences*, 108(36), 14,769– 14,774. https://doi.org/10.1073/pnas.1103910108

Lofton, D. D., Whalen, S. C., & Hershey, A. E. (2014). Effect of temperature on methane dynamics and evaluation of methane oxidation kinetics in shallow Arctic Alaskan lakes. *Hydrobiologia*, 721(1), 209– 222. https://doi.org/10.1007/s10750-013-1663-x

Lupascu, M., Wadham, J. L., Hornibrook, E. R. C., & Pancost, R. D. (2012). Temperature sensitivity of methane production in the permafrost active layer at Stordalen, Sweden: A comparison with non-permafrost northern wetlands. *Arctic, Antarctic, and Alpine Research*, 44(4), 469– 482. https://doi.org/10.1657/1938-4246-44.4.469

Malhotra, A., & Roulet, N. T. (2015). Environmental correlates of peatland carbon fluxes in a thawing landscape: Do transitional thaw stages matter? *Biogeosciences*, 12(10), 3119– 3130. https://doi.org/10.5194/bg-12-3119-2015

Malmer, N., Johansson, T., Olsrud, M., & Christensen, T. R. (2005). Vegetation, climatic changes and net carbon sequestration in a North-Scandinavian subarctic mire over 30 years. *Global Change Biology*, 11(11), 1895– 1909. https://doi.org/10.1111/j.1365-2486.2005.01042.x

Mastepanov, M., Sigsgaard, C., Dlugokencky, E. J., Houweling, S., Ström, L., Tamstorf, M. P., & Christensen, T. R. (2008). Large tundra methane burst during onset of freezing. *Nature*, 456(7222), 628– 630. https://doi.org/10.1038/nature07464

McCalley, C. K., Woodcroft, B. J., Hodgkins, S. B., Wehr, R. A., Kim, E.-H., Mondav, R., Crill, P. M., Chanton, J. P., Rich, V. I., Tyson, G. W., & Saleska, S. R. (2014). Methane dynamics regulated by microbial community response to permafrost thaw. *Nature*, 514(7523), 478– 481. https://doi.org/10.1038/nature13798

McGuire, A. D., Koven, C., Lawrence, D. M., Clein, J. S., Xia, J., Beer, C., Burke, E., Chen, G., Chen, X., Delire, C., Jafarov, E., MacDougall, A. H., Marchenko, S., Nicolsky, D., Peng, S., Rinke, A., Saito, K., Zhang, W., Alkama, R., Bohn, T. J., Ciais, P., Decharme, B., Ekici, A., Gouttevin, I., Hajima, T., Hayes, D. J., Ji, D., Krinner, G., Lettenmaier, D. P., Luo, Y., Miller, P. A., Moore, J. C., Romanovsky, V., Schädel, C., Schaefer, K., Schuur, E. A. G., Smith, B., Sueyoshi, T., & Zhuang, Q. (2016). Global biogeochemical cycles region between 1960 and 2009. *Global Biogeochemical Cycles*, 30, 1015– 1037. https://doi.org/10.1002/2016GB005405.Received

McGuire, A. D., Lawrence, D. M., Koven, C., Clein, J. S., Burke, E., Chen, G., Jafarov E., MacDougall A. H., Marchenko S., Nicolsky D., Peng S., Rinke A., Ciais P., Gouttevin I., Hayes D. J., Ji D., Krinner G., Moore J. C., Romanovsky V., Schädel C., Schaefer K., Schuur E. A. G., & Zhuang Q. (2018). Dependence of the evolution of carbon dynamics in the northern permafrost region on the trajectory of climate change. *Proceedings of the National Academy of Sciences*, 115(15), 3882– 3887. https://doi.org/10.1073/pnas.1719903115

Mekonnen, Z. A., Riley, W. J., & Grant, R. F. (2018). Accelerated nutrient cycling and increased light competition will lead to 21st century shrub expansion in North American Arctic Tundra. *Journal of Geophysical Research: Biogeosciences*, 123, 1683– 1701. https://doi.org/10.1029/2017JG004319

Mondav, R., Woodcroft, B. J., Kim, E.-H., McCalley, C. K., Hodgkins, S. B., Crill, P. M., Chanton, J., Hurst, G. B., VerBerkmoes, N. C., Saleska, S. R., Hugenholtz, P., Rich, V. I., & Tyson, G. W. (2014). Discovery of a novel methanogen prevalent in thawing permafrost. *Nature Communications*, 5(1), 3212. https://doi.org/10.1038/ncomms4212

Myhre, G., Shindell, D., Bréon, F.-M., Collins, W., Fuglestvedt, J., Huang, J., Koch, D., Lamarque, J.-F., Lee, D., Mendoza, B., Nakajima, T., Robock, A., Stephens, G., T, T., & Z, H. (2013). Anthropogenic and natural radiative forcing. In V. B, P. M. Midgley, T. F. Stocker, D. Qin, G.-K. Plattner, M. Tignor, S. K. Allen, J. Boschung, A. Nauels, & Y. Xia (Eds.), *Climate Change 2013 the Physical Science Basis: Working Group I Contribution to the Fifth Assessment Report of the Intergovernmental Panel on Climate Change* (pp. 659– 740). Cambridge, UK and New York: Cambridge University Press. https://doi.org/10.1017/CBO9781107415324.018

Neubauer, S. C., & Megonigal, J. P. (2015). Moving beyond global warming potentials to quantify the climatic role of ecosystems. *Ecosystems*, 18(6), 1000– 1013. https://doi.org/10.1007/s10021-015-9879-4

Olefeldt, D., & Roulet, N. T. (2012). Effects of permafrost and hydrology on the composition and transport of dissolved organic carbon in a subarctic peatland complex. *Journal of Geophysical Research*, 117, G01005. https://doi.org/10.1029/2011JG001819

Olefeldt, D., Turetsky, M. R., Crill, P. M., & Mcguire, A. D. (2013). Environmental and physical controls on northern terrestrial methane emissions across permafrost zones. *Global Change Biology*, 19(2), 589– 603. https://doi.org/10.1111/gcb.12071

Penger, J., Conrad, R., & Blaser, M. (2012). Stable carbon isotope fractionation by methylotrophic methanogenic archaea. *Applied and Environmental Microbiology*, 78(21), 7596– 7602. https://doi.org/10.1128/AEM.01773-12

Rydén, B. E., & Kostov, L. (1980). Thawing and freezing in tundra soils. *Ecological Bulletins*, 30, 251– 281. Retrieved from http://www.jstor.org/stable/20112776

Schädel, C., Bader, M. K.-F., Schuur, E. A. G., Biasi, C., Bracho, R., Čapek, P., de Baets, S., Diáková, K., Ernakovich, J., Estop-Aragones, C., Graham, D. E., Hartley, I. P., Iversen, C. M., Kane, E., Knoblauch, C., Lupascu, M., Martikainen, P. J., Natali, S. M., Norby, R. J., O'Donnell, J. A., Chowdhury, T. R., Šantrůčková, H., Shaver, G., Sloan, V. L., Treat, C. C., Turetsky, M. R., Waldrop, M. P., & Wickland, K. P. (2016). Potential carbon emissions

dominated by carbon dioxide from thawed permafrost soils. *Nature Climate Change*, 6(10), 950– 953. https://doi.org/10.1038/nclimate3054

Schuur, E. A. G., McGuire, A. D., Grosse, G., Harden, J. W., Hayes, D. J., Hugelius, G., Koven, C. D., Kuhry, P., Lawrence, D. M., Natali, S. M., Olefeldt, D., Romanovsky, V. E., Schaefer, K., Turetsky, M. R., Treat, C. C., & Vonk, J. E. (2015). Climate change and the permafrost carbon feedback. *Nature*, 520(7546), 171– 179. https://doi.org/10.1038/nature14338

Schuur, E. A. G., McGuire, A. D., Romanovsky, V., Schädel, C., & M., M. (2018). Chapter 11: Arctic and boreal carbon. In Second State of the Carbon Cycle Report (SOCCR2): A Sustained Assessment Report. In and Z. Z. Cavallaro, N. G. Shrestha, R. Birdsey, M. A. Mayes, R. G. Najjar, S. C. Reed, P. Romero-Lankao (Eds.) (pp. 428– 468). Washington, DC: U.S. Global Change Research Program. https://doi.org/10.7930/%0ASOCCR2.2018.Ch11

Sonesson, M. (1972). Primary production studies, Stordalen 1971. Cryptogams. In *International Biological Programme, Swedish Tundra Biome Project Technical report* (Vol. 9, pp. 18– 23). Stockholm: Swedish Natural Science Research Council.

Thauer, R. K., Kaster, A. K., Seedorf, H., Buckel, W., & Hedderich, R. (2008). Methanogenic archaea: Ecologically relevant differences in energy conservation. *Nature Reviews Microbiology*, 6(8), 579– 591. https://doi.org/10.1038/nrmicro1931

van den Hurk, B., Kim, H., Krinner, G., Seneviratne, S. I., Derksen, C., Oki, T., Douville, H., Colin, J., Ducharne, A., Cheruy, F., Viovy, N., Puma, M. J., Wada, Y., Li, W., Jia, B., Alessandri, A., Lawrence, D. M., Weedon, G. P., Ellis, R., Hagemann, S., Mao, J., Flanner, M. G., Zampieri, M., Materia, S., Law, R. M., & Sheffield, J. (2016). LS3MIP (v1.0) contribution to CMIP6: The Land Surface, Snow and Soil moisture Model Intercomparison Project – Aims, setup and expected outcome. *Geoscientific Model Development*, 9(8), 2809– 2832. https://doi.org/10.5194/gmd-9-2809-2016

Wania, R., Melton, J. R., Hodson, E. L., Poulter, B., Ringeval, B., Spahni, R., Bohn, T., Avis, C. A., Chen, G., Eliseev, A. V., Hopcroft, P. O., Riley, W. J., Subin, Z. M., Tian, H., van Bodegom, P. M., Kleinen, T., Yu, Z. C., Singarayer, J. S., Zürcher, S., Lettenmaier, D. P., Beerling, D. J., Denisov, S. N., Prigent, C., Papa, F., & Kaplan, J. O. (2013). Present state of global wetland extent and wetland methane modelling: Methodology of a model inter-comparison project (WETCHIMP). *Geoscientific Model Development*, 6(3), 617– 641. https://doi.org/10.5194/gmd-6-617-2013

Woodcroft, B. J., Singleton, C. M., Boyd, J. A., Evans, P. N., Emerson, J. B., Zayed, A. A. F., Hoelzle, R. D., Lamberton, T. O., McCalley, C. K., Hodgkins, S. B., Wilson, R. M., Purvine, S. O., Nicora, C. D., Li, C., Frolking, S., Chanton, J. P., Crill, P. M., Saleska, S. R., Rich, V. I., & Tyson, G. W. (2018). Genome-centric view of carbon processing in thawing permafrost. *Nature*, 560(7716), 49– 54. https://doi.org/10.1038/s41586-018-0338-1

Xu, X., Yuan, F., Hanson, P. J., Wullschleger, S. D., Thornton, P. E., Riley, W. J., Song, X., Graham, D. E., Song, C., & Tian, H. (2016). Reviews and syntheses: Four decades of modeling methane cycling in terrestrial ecosystems. *Biogeosciences*, 13(12), 3735– 3755. https://doi.org/10.5194/bg-13-3735-2016

Ye, R., Jin, Q., Bohannan, B., Keller, J. K., McAllister, S. A., & Bridgham, S. D. (2012). pH controls over anaerobic carbon mineralization, the efficiency of methane production, and methanogenic pathways in peatlands across an ombrotrophic–minerotrophic gradient. *Soil Biology and Biochemistry*, 54, 36–47. https://doi.org/10.1016/j.soilbio.2012.05.015

Yvon-Durocher, G., Allen, A. P., Bastviken, D., Conrad, R., Gudasz, C., St-Pierre, A., Thanh-Duc, N., & del Giorgio, P. A. (2014). Methane fluxes show consistent temperature dependence across microbial to ecosystem scales. *Nature*, 507(7493), 488– 491. https://doi.org/10.1038/nature13164

Zheng, J., RoyChowdhury, T., Yang, Z., Gu, B., Wullschleger, S. D., & Graham, D. E. (2018). Impacts of temperature and soil characteristics on methane production and oxidation in Arctic tundra. *Biogeosciences*, 15(21), 6621–6635. https://doi.org/10.5194/bg-15-6621-2018